CREAT. MATH. INFORM.
Volume **29** (2020), No. 1,
Pages 101 - 108

Online version at https://creative-mathematics.cunbm.utcluj.ro/
Print Edition: ISSN 1584 - 286X; Online Edition: ISSN 1843 - 441X
DOI: https://doi.org/10.37193/CMI.2020.01.12

New ant colony optimization algorithm in medical images edge detection

CRISTINA ŢICALĂ and IOANA ZELINA

ABSTRACT. In this paper we aim to use a demicontractive operator in terms of admissible perturbations in an ant colony optimization (ACO) algorithm for edge detection of medical images. Two admissible perturbations are used. Practical results are presented. Comparison with results using different operators are made.

1. INTRODUCTION

Ant colony optimization algorithms are inspired by nature, based on the behavior of real ant colonies, in which ants deposit pheromone on the ground, in order to mark favorable paths in their search for food. These paths will be followed by the members of the colony. The first Ant Colony algorithm, called Ant Colony System was proposed by Dorigo et all [3]. From that point on a large number of algorithms based on ACO were developed.

In this paper ACO is introduced to approach medical images edge detection problem, where the aim is to extract the edge of the image, since the edge is decisive to understand the image content. The new feature of this algorithm is the admissible perturbations applied to a demicontractive operator.

Definition 1.1. [5] We say that $T : C \to C$, where C is subset of $\mathbb{R}$, is *demicontractive* if there exists a constant $k < 1$ such that, for each fixed point p of T and each $x \in C$,

$$\|Tx - p\|^2 \leq \|x - p\|^2 + k\|x - Tx\|^2. \tag{1.1}$$

We call k the *contraction coefficient*.

Example 1.1. [4] An example of demicontractive mapping is $T : \mathbb{R} \to \mathbb{R}$, defined by

$$Tx = \begin{cases} \frac{2}{3}x \sin \frac{1}{x}, \text{ if } x \neq 0 \\ 0, \text{ if } x = 0 \end{cases} \tag{1.2}$$

The theory of admissible perturbations of an operator introduced by Rus in [8], opened a new direction of research and unified the most important aspects of the iterative approximation of fixed point for single valued self operators.

Definition 1.2. [8] Let X be a nonempty set. A mapping $G : X \times X \to X$ is called admissible if it satisfies the following two conditions:
$(A1)$ $G(x, x) = x$, for all $x \in X$;
$(A2)$ $G(x, y) = x$ implies $y = x$.

Let $f : X \to X$ be an operator. Then we consider the operator $f_G : X \to X$ defined by

$$f_G(x) := G(x, f(x)).$$

Received: 03.10.2019. In revised form: 13.12.2019. Accepted: 10.01.2020
2010 *Mathematics Subject Classification.* 47H10, 47H09, 97R40.
Key words and phrases. *Fixed point, Krasnoselskij iteration, Admissible perturbation, Ant Colony Optimization.*
Corresponding author: Cristina Ţicală; cristina.ticala.pop@gmail.com

Definition 1.3. [8] Let $f : X \to X$ a nonlinear operator and $G : X \times X \to X$ be an admissible mapping. The iterative algorithm $\{x_n\}$ given by $x_0 \in X$ and

$$x_{n+1} = G\left(x_n, f\left(x_n\right)\right),\ n \geq 0. \tag{1.3}$$

is called the *Krasnoselskij algorithm* corresponding to G, or the *GK-algorithm*.

Example 1.2. Let $(V, +, \mathbb{R})$ be a real vector space, $X \subset V$ a convex subset, $\lambda \in (0, 1)$, $f : X \to X$ and $G : X \times X \to X$ defined by

$$G\left(x, f\left(x\right)\right) := \left(1 - \lambda\right) x + \lambda f\left(x\right),\ x \in X. \tag{1.4}$$

Then f_G is admissible perturbation of f, perturbation called the Krasnoselskij perturbation of f.

Example 1.3. Let $(V, +, \mathbb{R})$ be a vectorial space, $X \subset V$ a convex subset, $\chi : X \times X \to (0, 1)$, $f : X \to X$ şi $G : X \times X \to X$ defined by

$$G\left(x, y\right) := \left(1 - \chi\left(x, y\right)\right) x + \chi\left(x, y\right) y. \tag{1.5}$$

Then f_G is an admissible perturbation of f.

The admissible perturbation operator was studied in various papers such as [1], [2], [9], [11], [10].

In this paper we aim to use a demicontractive operator in terms of admissible perturbations in an ant colony optimization (ACO) algorithm for edge detection of medical images. Two admissible perturbations are used in computing the heuristic value required in ACO algorithm. Practical results are obtained using various medical images shown in figure 3. Execution times for each image and each edge extracting method are presented. Comparison with results using different operators are made.

2. Ant colony optimization

The ACO algorithm builds the optimal solution of the target problem using artificial ants that search the best path, iteratively and controlled, in the search space, depositing pheromones while searching. In other words, assuming that there are K ants engaged in the search, in a space $\mathcal{X}$, which consists of $M_1 \times M_2$ nodes, ACO may be summarized as described by Tian et all in [6]:

- Initiate all K ants and the pheromone matrix, $\tau^{(0)}$;
- For every solution construction step index $n = 1 : N$
  - for every ant $k = 1 : K$
    - ⋆ Consecutively move the k-th for L steps according with a transition probability matrix;
  - update the pheromone matrix $\tau^{(n)}$;
- Make the solution decision according to the final pheromone matrix $\tau^{(N)}$.

There are two fundamental problems ACO has to solve which are: to build the transition probability matrix $p^{(n)}$, and to update the pheromone matrix $\tau^{(n)}$. Each problem will be presented in this paper.

At the n-th construction step, the k-th ant is moving from the node I to the node J according to a transition probability given by:

$$p_{IJ}^{n} = \frac{\left(\tau_{IJ}^{(n-1)}\right)^{\alpha} \left(\eta_{IJ}\right)^{\beta}}{\sum_{J \in \Omega_I} \left(\tau_{IJ}^{(n-1)}\right)^{\alpha} \left(\eta_{IJ}\right)^{\beta}}, \qquad \text{if } J \in \Omega_I, \tag{2.6}$$

where $\tau_{IJ}^{(n-1)}$ is the existing pheromone value on the arc which connects the nodes I and J, at construction step $n-1$; η_{IJ} is the heuristic value on the arc which connects the nodes I and J, value that is the same for all the N construction steps; α, β are weighting factors for the pheromone and the heuristic respectively; Ω_I is the 8-connectivity neighborhood of node I, for each node of the space.

The information in the pheromone matrix is updated twice during ACO: first after each ant moves within each construction step, and second update is performed after the move of all K ants within each construction step. The first update is performed after the move of the k-th ant in the n-th construction step according to [6].

$$\tau_{IJ}^{(n)} = \begin{cases} \tau_{IJ}^{n-1} \cdot (1-\rho) + \rho \cdot \Delta_{IJ}^{(k)}, & \text{if } (I,J) \text{ is on the best path} \\ \tau_{IJj}^{(n-1)}, & \text{otherwise .} \end{cases} \tag{2.7}$$

where ρ is the pheromone evaporation rate, $\Delta_{IJ}^{(k)}$ is the quantity of pheromone laid on edge (I,J) by ant k. Furthermore, the best path is an user defined criterion; it can be the best path found in the current construction step, or from the start of ACO algorithm, or a combination of these two.

The second update is performed using a procedure suggested in [3], as

$$\tau^{(n)} = (1-\psi) \cdot \tau^{(n-1)} + \psi \cdot \tau^{(0)}; \tag{2.8}$$

where ψ the pheomone decay rate.

3. ACO ALGORITHM - FOR EDGE DETECTION IN MEDICAL IMAGES

The proposed edge detection algorithm uses artificial ants which move in a bi-dimensional image in order to build the pheromone matrix, each element represents the edge information for every pixel in the image.

The proposed approach starts with the initialization process, runs for N steps to create and update the pheromone matrix, and last, performs the decision process to determine the edge of the image.

3.1. **Initialization process.** In the initialization process all the K ants are placed randomly in the image. Each pixel of the image is viewed as a node. Each value of the initial pheromone matrix $\tau_{(0)}$ is set to a constant τ_{init}.

3.2. **Construction process.** At the n-th construction step, $n = \overline{1,N}$, one ant is randomly chosen from all K ants and this ant will be consecutively moving for L steps. The ant will move from node I to J according to the transition probability in (2.6).

There are two crucial aspects in the construction process. First, it is the issue of establishing the heuristic η_{ij} from (2.6). In this paper, we propose to compute the heuristic value according to the local statistic of the pixel $I_{i,j}$.

$$\eta_{i,j} = \frac{1}{Z} V_c(I_{i,j}), \tag{3.9}$$

where $Z = \sum_{i=1,M_1} \sum_{1,M_2} V_c I_(i,j)$, is a normalization factor, $I_{i,j}$ is the intensity value of the pixel at the position (i,j) from the image, $V_c(I_{i,j})$ is a function which processes the "clique" $cI_{i,j}$ defined in [6], figure 2. The value of $V_c(I_{i,j})$ depends on the variation of image's intensity values on $cI_{i,j}$. More specifically, the value of $V_c(I_{i,j})$ at the pixel $I_{i,j}$ according to [6] is

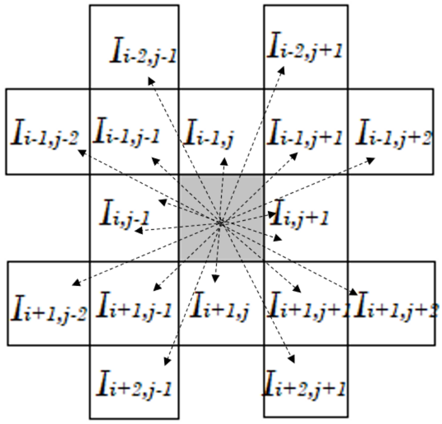

FIGURE 1. Local configuration at $I_{i,j}$ pixel, for computing the variation value $V_c(I_{i,j})$ defined by (3.10). The pixel $I_{i,j}$ is the gray square.

$$\begin{aligned} V_c(I_{i,j}) = \quad & f\left(|I_{i-2,j-1} - I_{i+2,j+1}| + |I_{i-2,j+1} - I_{i+2,j-1}|\right. \\ & + |I_{i-1,j-2} - I_{i+1,j+2}| + |I_{i-1,j-1} - I_{i+1,j+1}| \\ & + |I_{i-1,j} - I_{i+1,j+1}| + |I_{i-1,j+1} - I_{i+1,j-1}| \\ & \left. + |I_{i-1,j+2} - I_{i+1,j-2}| + |I_{i,j-1} - I_{i,j+1}|\right). \end{aligned} \tag{3.10}$$

In this paper, the considered operators for $f(\cdot)$ from (3.10) are listed below.

$$f(x) = \lambda x^2, \text{ for } x \geq 0, \tag{3.11}$$

$$f(x) = \begin{cases} \sin\left(\dfrac{\pi x}{2\lambda}\right), & 0 \leq x \leq \lambda; \\ 0, & \text{otherwise.} \end{cases} \tag{3.12}$$

$$f(x) = \begin{cases} (1-\lambda)\cdot x + \lambda \cdot \frac{2}{3} x \sin\frac{1}{x} & \text{if } x \neq 0; \\ 0, & \text{if } x = 0. \end{cases} \tag{3.13}$$

$$f(x) = \begin{cases} \left(1 - \chi\left(x, \frac{2}{3}x\sin\frac{1}{x}\right)\right)x + \chi\left(x, \frac{2}{3}x\sin\frac{1}{x}\right)\cdot\frac{2}{3}x\sin\frac{1}{x} & \text{if } x \neq 0 \\ 0 & \text{if } x = 0. \end{cases} \tag{3.14}$$

where $\chi : \mathbb{R} \times \mathbb{R} \longrightarrow [0,1)$,

$$\chi(x,y) = \frac{x^2 \cdot y^2}{(1+x^2)\cdot(1+y^2)}. \tag{3.15}$$

The parameter λ from the equations (3.11) and (3.12) adjusts the shape of the operators.

During the conducted research about admissible perturbations of demicontractive operators, using Krasnoselskij perturbation on the demicontractive operator (1.2), the operator given by (3.13) was obtained. It was established that (3.13) can be used as test function to construct the heuristic value in this algorithm. This operator has not been used before in this form, or in edge detection algorithms.

Also, continuing the research, we considered the operator admissible perturbation defined in [8] by (1.4).

The operator listed in (3.14) is an admissible perturbation operator obtained by applying the function χ defined by (3.15) to demicontractive operator stated in (1.2).

The first two operators (3.11), (3.12), are test functions used in [6]. We used these operators in order to evaluate the results obtained with the proposed admissible perturbation operators defined in (3.13) and (3.14).

The second aspect is establishing the domain in which one ant found in node (l, m) can make moves, i.e. $\Omega_{l,m}$ from (2.6). In this paper an 8-connectivity domain is considered, figure 2.

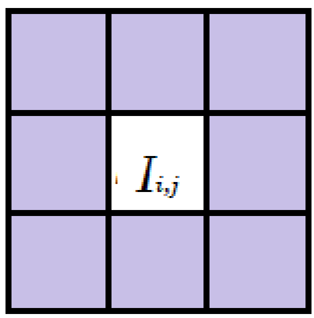

FIGURE 2. 8-connectivity neighborhood for the pixel $I_{i,j}$ (marked as gray regions)

3.3. **Update process.** The algorithm uses two update operations for the pheromone matrix. First update is made after each ant moves within each construction step. Each element of the matrix is updated according to (3.16)

$$\tau_{i,j}^{(n)} = \begin{cases} \tau_{ij}^{n-1} \cdot (1-\rho) + \rho \cdot \Delta_{ij}^{(k)}, & \text{if } I_{i,j} \text{ is visited by the current ant;} \\ \tau_{ij}^{(n-1)}, & \text{otherwise.} \end{cases} \tag{3.16}$$

The second update is made after the movement of all ants within each construction step according to

$$\tau^{(n)} = (1-\psi) \cdot \tau^{(n-1)} + \psi \cdot \tau^{(0)}; \tag{3.17}$$

where ψ is the pheromone decay rate.

3.4. **Decision process.** At this point of the algorithm a binary decision is made for each pixel in order to establish if it is edge or not, by applying a threshold T on the final pheromone matrix $\tau^{(N)}$. The threshold is computed as stated by Doringo et all in [7].

4. Results

We tested the algorithm on four medical images which are shown in figure 3. Also we used all the parameters values used in [6].

Experimental results are presented next. We provided the images with the determined edge using each operator from (3.11) - (3.14)

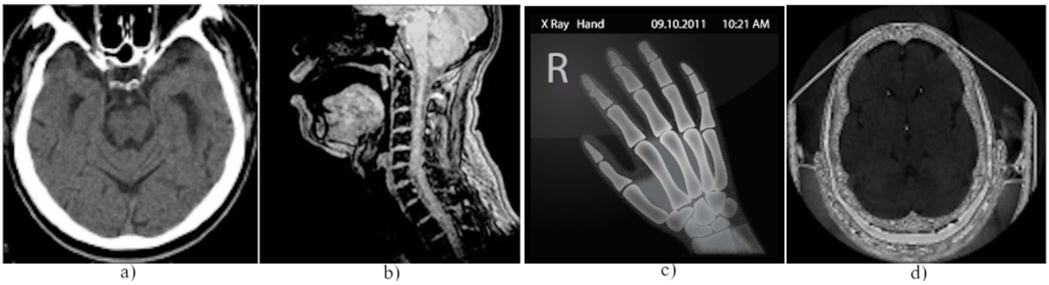

FIGURE 3. Test images: *a) Brain CT (126 $\times$ 128); b) Cervical CT (225 $\times$ 225), c) Hand X-ray (225 $\times$ 225), d) Head CT (128 $\times$ 128)*

FIGURE 4. Various edges of *Brain CT* obtained using: a) operator (3.11), b) operator (3.12), c) operator (3.13), d) operator (3.14).

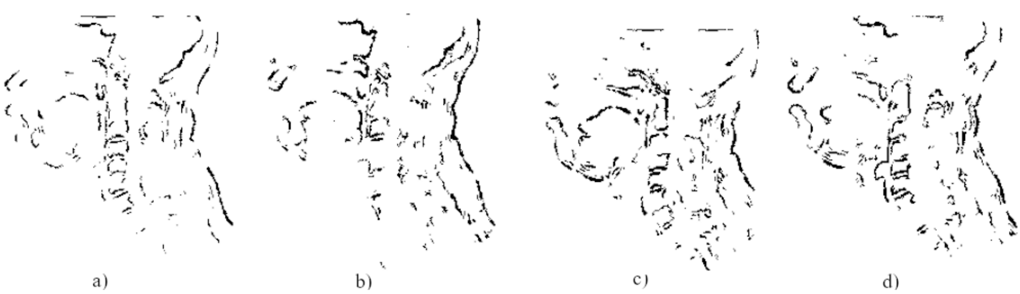

FIGURE 5. Various edges of *Cervical CT* obtained using: a) operator (3.11), b) operator (3.12), c) operator (3.13), d) operator (3.14).

The execution time for each of the four images using operators (3.11), (3.12), (3.13), (3.14) are shown in the next table.

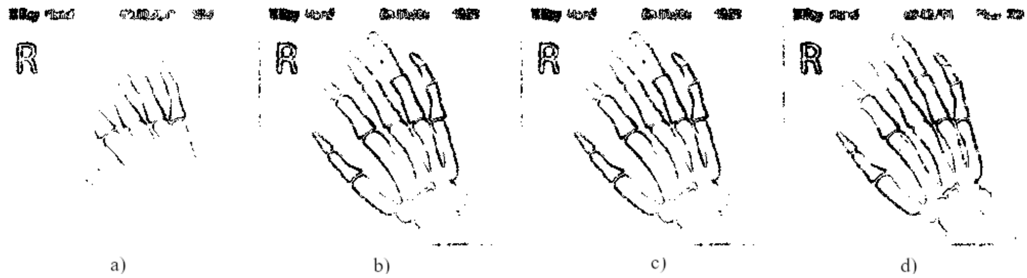

FIGURE 6. Various edges of *Hand X-ray* obtained using: a) operator (3.11), b) operator (3.12), c) operator (3.13), d) operator (3.14).

FIGURE 7. Various edges of *Head CT* obtained using: a) operator (3.11), b) operator (3.12), c) operator (3.13), d) operator (3.14).

	$Operator$ (3.3)	$Operator$ (3.4)	$Operator$ (3.5)	$Operator$ (3.6)
$Brain\ CT$	47.2442	47.0982	48.2437	47.0464
$Cervical\ CT$	138.9476	139.8230	140.2909	126.6480
$Hand\ X-ray$	189.3574	204.5009	202.6446	185.6683
$Head\ CT$	38.8062	29.5953	38.6136	41.5907

5. CONCLUSIONS AND FURTHER WORK

The ACO-based edge detection approach is implemented using the Matlab programming language and run on a PC - AMD Rysen 5 2500U, 2GHz. As one can see, the execution time for various methods are close. The dimension of the image is very important for the execution time. The results obtained with various methods were comparable.

It was necessary to establish how close were the results obtained with various operators, since we wanted to know if demicontractive operators can be used in edge detection algorithms. Consequently counting were made.

We found that in the Krasnoselskij perturbation operator (3.13) edge image there are: 740 pixels not in the edge image obtained with (3.11); 593 pixels not in the edge image obtained with (3.12); 677 pixels not in the edge image obtained with (3.14).

On the other hand we can see that the edge information obtained with operator (3.12) seems to have more pixels on the edge; thus we made the counting the other way around. There were a number of pixels which were not on the edge for operator (3.13) but found by operators (3.11), (3.12), (3.14) as it follows: 400, 696, 657 respectively.

The same counting was made for operator (3.14) regarding operators (3.11) and (3.12). We found more 637 respectively 556 pixels on the edge determined by "χ"-perturbation, (3.14), than the mentioned operators. And we found a number of 317 pixels and 679 pixels found by (3.11) and (3.12) respectively but not found by "χ"-perturbation.

This counting was performed on the rest of the images. Each time there were pixels "seen" with one operator and disregarded by the others. This fact leads to the idea of building a new edge which includes all the edge information obtained with each of four methods, for every image. We applied this idea and the result is presented in figure 8.

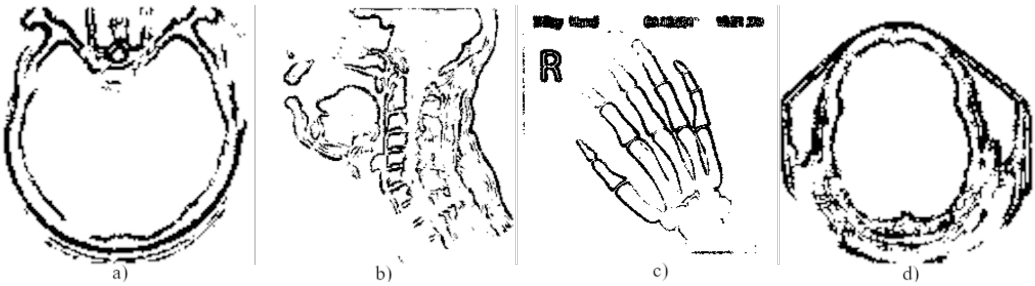

FIGURE 8. New edges: a) Brain CT b) Cervical CT c) Hand X-ray d) Head CT

Further work shall include modification of the update process for the pheromone matrix, and improvements of the communication between ants.

REFERENCES

[1] Berinde, V., *Convergence theorems for fixed point iterative methods defined as admissible perturbations of a nonlinear operator*, Carpathian J. of Math., **29** (2013), No. 1, 9–18

[2] Berinde, V., Khan, A. R. and Fukhar-ud din, H., *Fixed point iterative methods defined as admissible perturbations of generalized pseudocontractive operators*, J. Nonlinear Convex Anal., **16** (2015), No. 3, 563–572

[3] Dorigo, M. and Stützle, T., *Ant Colony Optimization*, MIT Press, Cambridge, MA, 2004

[4] Chidume, C. and Măruşter, Ş., *Iterative methods for the computation of fixed points of demicontractive mappings*, J. Comput. Appl. Math., **234** (2010), 861–882

[5] Hicks, T. L. and Kubicek, J. D., *On the Mann iteration in a Hilbert space*, J. Math. Anal. Appl., **59** (1977), 498–504

[6] Tian, J., Yu, W. and Xie, Sh., *An ant colony optimization algorithm for image edge detection*, 2008 IEEE Congress on Evolutionary Computation (IEEE World Congress on Computational Intelligence), June 2008, pp. 751–756

[7] Otsu, N., *A threshold selection method from gray-level histograms*, IEEE Trans. Syst. Man Cybern., **9** (1979), No. 1, 62–66

[8] Rus, I. A., *An abstract point of view on iterative approximation of fixed points*, Fixed Point Theory, **33** (2012), 179–192

[9] Ţicală, C., *Approximating solutions of generalized pseudocontractive variational inequalities by admissible perturbation type iterative methods*, Creative Math. & Inf., **22** (2013), No. 2, 237–241

[10] Ţicală, C., *Approximating fixed points of demicontractive mappings by iterative methods defined as admissible perturbations*, Creative Math. & Inf., **25** (2016), No. 1, 121–126

[11] Ţicală, C., *A weak convergence theorem for a Krasnoselskij type fixed point iterative method in Hilbert spaces using an admissible perturbation*, SSRSMI, **25** (2015), No. 1, 243–252

DEPARTMENT OF MATHEMATICS AND COMPUTER SCIENCE
TECHNICAL UNIVERSITY OF CLUJ-NAPOCA
NORTH UNIVERSITY CENTRE AT BAIA MARE
VICTORIEI 76, 430122 BAIA MARE, ROMANIA
Email address: cristina.ticala@cunbm.utcluj.ro
Email address: ioanazelina@yahoo.com